Characterization and Properties of Manganese Oxide Coated Zeolite as Adsorbent for Removal of Copper(II) and Lead(II) Ions from Solution

Weihua Zou,[†,‡] Runping Han,*[,‡] Zongzhang Chen,*[,†] Jie Shi,[‡] and Liu Hongmin[‡]

School of Chemistry and Chemical Engineering, Hunan University, The Yuelu Mountain of Changsha, Hunan Province, 410082, People's Republic of China, and Department of Chemistry, Zhengzhou University, No 75 of Daxue North Road, Zhengzhou, Henan Province, 450052, People's Republic of China

A new adsorbent, manganese oxide coated zeolite (MOCZ), was characterized and employed for the removal of Cu(II) and Pb(II) from aqueous solution using batch equilibrium experiments. Scanning electron microscope (SEM), X-ray photoelectron spectroscopy (XPS), and BET analyses were used to observe the surface properties of the coated layer. Binding of Cu(II) and Pb(II) ions by MOCZ was clearly pH-dependent, and the loading capacities increased with increasing pH. Adsorption behavior of Cu(II) and Pb(II) ions can be approximately described with the Langmuir and Redlich−Peterson equation. The thermodynamic parameters ($\Delta G°$, $\Delta H°$, and $\Delta S°$) were also determined, and the adsorption process is more favored at higher temperatures.

1. Introduction

To remove heavy metals effectively from metal-laden wastewater, various processes and measurements for the treatment and disposal of metal-containing wastewaters have been developed, such as chemical precipitation, ion exchange, membrane separation, and activated carbon adsorption.[1] However, most of these methods suffer from some drawbacks in that they may be ineffective, be expensive, generate secondary pollution, or be ineffective at low metal concentrations. Hence, there is a crucial need for the development of a method that is not only cost-effective and economic but can also be easily implemented. This leads to a search for cheaper, easily obtainable materials for the adsorption of heavy metals. Some natural materials such as zeolites, chitosan, and clay are being considered as alternative low-cost adsorbents.[2] While their sorption capacity is usually less than those of synthetic or modified adsorbents, these minerals could provide inexpensive substitutes for the treatment of heavy metal-laden wastewaters. To enhance the sorption capacity of natural adsorbents to adsorb heavy metals, many attempts have been made to chemically modify their surface using metal oxides. [3,4,5]

Zeolites are aluminosilicate minerals containing exchangeable alkali and alkaline earth metal cations (normally Na, K, Ca, and Mg) as well as water in their structural framework. The physical structure is porous, enclosing interconnected cavities in which the metal ions and water molecules are contained.[6] Zeolites represent an appropriate material for removing heavy metal ions from wastewater because of their relatively low price coupled with the fact that their exchangeable ions (Na^+, Ca^{2+}, and K^+) are relatively harmless. To improve the medias performance (such as sorption capacity, increased mechanical strength, and resistance to chemical environments), several methods have been used to modify zeolites by either physical or chemical modification.

Manganese oxides are typically thought to be the most important scavengers of aqueous trace metals in soil, sediments, and rocks through their seemingly dominant sorptive behavior. Crystalline manganese oxides generally have either a layered structure (e.g., birnessite and vernadite) or a tunneled structure (such as pyrolusite and hollandite), but manganese oxides found in soils are typically amorphous.[7] They have a large surface area, microporous structure, and high affinity for metal ions [8,9,10,11] (such as Pb, Cu, Cd, Zn, and UO_2^{2+}), providing an efficient scavenging pathway for heavy metals in toxic systems. Manganese dioxides is one kind of surface acidic oxides, whose pH_{pzc} (point of zero charge) value is about 2.0 to 4.5 and the typical pzc of birnssite ranges from 1.5 to 2.8.[12,13] The charge of the hydrous oxide depends on the pH of the medium. Commonly, the surface charge of manganese oxides is negative, and they can be used as adsorbents to remove heavy metals from wastewater. However, pure manganese oxide as a filter media is not favorable for both economic reasons and unfavorable physical and chemical characteristics, but coating manganese oxide to a media surface may provide an effective surface and may be a promising media for heavy metal removal from wastewater.

The research described here was designed to investigate characteristics of manganese oxide coated zeolite (MOCZ) and to test the properties of MOCZ as an adsorbent for removing copper(II) and lead(II) from synthetical solutions using a batch system. SEM/EDAX and BET analysis were employed to examine the properties of adsorption reactions for Cu(II) and Pb(II) ions on MOCZ in water. The influence of experimental conditions such as pH, contact time, temperature, and initial concentration have been studied. The experimental data were fitted into Langmuir, Freundlich, Temkin, and Reldich−Peterson equations to determine which isotherm gives the best correlation to experimental data, and the adsorption capacities of MOCZ were also examined using the adsorption isotherm technique. The kinetic and thermodynamic parameters such as $\Delta G°$, $\Delta H°$, $\Delta S°$, E_a, k_1, k_2, etc. were also calculated to determine rate constants and the adsorption mechanism.

* Corresponding authors. E-mail: rphan67@zzu.edu.cn (R.H.); whzou@zzu.edu.cn (Z.C.). Fax: +86 371 67763220.
† Hunan University.
‡ Zhengzhou University.

10.1021/je0504008 CCC: $33.50
Published on Web 02/16/2006

Equilibrium isotherms are measured to determine the capacity of the adsorption of the sorbent for metal ions. Four adsorption models (the Langmuir, Freundlich, Temkin, and Redlich−Peterson isotherms) were used to describe the equilibrium between adsorbed metal ions on MOCZ and metal ions in solution at a constant temperature.

The most widely used isotherm equation for modeling equilibrium data is the Langmuir model.[14] The isotherm is valid for monolayer adsorption onto a surface containing a finite number of identical sites. It can be described by the linearized form:

$$C_e/q_e = 1/(K_a q_{max}) + C_e/q_{max} \quad (1)$$

where q_{max} (mmol·g^{-1}) is the maximum amount of metal ion per unit weight of MOCZ and K_a(L·mmol^{-1}) is the equilibrium adsorption constant. C_e is the equilibrium metal ion concentration in mmol·L^{-1} and q_e is the adsorption equilibrium metal ion uptake capacity in mmol·g^{-1}. By plotting C_e/q_e versus C_e, q_{max} and K_a can be determined.

The Freundlich expression is an empirical equation describing sorption onto a heterogeneous surface. The Freundlich equation is commonly presented as[15]

$$q_e = K_F C_e^{1/n} \quad (2)$$

and the equation may be linearized by taking logarithms

$$\ln q_e = \ln K_F + 1/n \ln C_e \quad (3)$$

where q_e is the amount of solute adsorbed per unit weight of adsorbent (mmol·g^{-1}), C_e is the equilibrium concentration of solute in the bulk solution (mmol·L^{-1}), K_F (mmol·g^{-1}) and $1/n$ are the Freundlich constants related to the adsorption capacity and sorption intensity of the sorbent, respectively.

The Temkin isotherm equation is as follows:[16]

$$q_e = RT \ln(a_t C_e)/b_t \quad (4)$$

The linear form of Temkin isotherms can be expressed by

$$q_e = A + B \ln C_e \quad (5)$$

where R is the general gas constant; T is absolute temperature (K); and a_t and b_t represent isotherm constants, respectively. A [$= (RT \ln a_t)/b_t$] and B ($= RT/b_t$) represent isotherm constants, respectively. The constant B is related to the heat of adsorption.

The Redlich−Peterson isotherm[17] contains three parameters, and the form of equation includes features of the Langmuir and the Freundlich isotherms. It can be described as follows:

$$q_e = K_{RP} C_e/(1 + a_{RP} C_e^{\,g}) \quad (6)$$

This equation can be converted to a linear form by taking logarithms:

$$\ln(K_{RP} C_e/q_e - 1) = g \ln C_e + \ln a_{RP} \quad (7)$$

These three isotherm constants, namely, K_{RP}, a_{RP}, and g ($0 < g < 1$), can be evaluated from the linear plot represented by eq 7 using a trial and error optimization method.

Thermodynamic parameters including free energy change ($\Delta G°$), enthalpy change ($\Delta H°$), and entropy change ($\Delta S°$) can be determined from the change in equilibrium constants with temperature. The free energy ($\Delta G°$) of the sorption reaction, considering the sorption equilibrium constant (K_a), is given by the following equation:[18]

$$\Delta G° = -RT \ln K_a \quad (8)$$

The enthalpy ($\Delta H°$) and entropy ($\Delta S°$) can be obtained from the slope and intercept of the van't Hoff equation of $\Delta G°$ versus T as follows:

$$\Delta G° = \Delta H° - T\Delta S° \quad (9)$$

where R is the gas constant, 8.314 J·mol^{-1}·K^{-1}, and T is absolute temperature, K.

2. Materials and Methods

2.1. Preparation of MOCZ. The raw zeolites samples used in this study were obtained from Xinyang City in China. Before use, the zeolites were crushed and sieved through mesh screens, and a fraction of the particles of average size were soaked in tap water for 24 h to decrease their alkalescence, rinsed with distilled water, and dried at 373 K in an oven in preparation for surface coating. MOCZ were accomplished by utilizing a reductive procedure modified to precipitate colloids of manganese oxides on the media surface. A boiling solution containing potassium permanganate was poured over dried zeolites placed in a beaker, and then hydrochloric acid (37.5 %, w_{HCl}/w_{H_2O}) was added dropwise into the solution. After stirring for 1 h, the media was filtered, washed to pH 7.0 using distilled water, dried at room temperature, and stored in a polypropylene bottle for use.

The removal capacity of MOCZ was compared with that of raw zeolite. The maximum adsorption capacities for zeolite and MOCZ were found to be 0.061 mmol·g^{-1} zeolite and 0.108 mmol·g^{-1} MOCZ for Cu(II), respectively. Adsorption capacities for Pb(II) were 0.134 mmol·g^{-1} zeolite and 0.243 mmol·g^{-1} MOCZ, respectively. The results indicated that the adsorption capacity of MOCZ are nearly one time more than that of raw zeolite for the removal of Cu(II) and Pb(II).

2.2. Metal Solution. All chemicals and reagents used for experiments and analyses were of analytical grade. Stock solutions of 2000 mg·L^{-1} Pb(II) and Cu(II) were prepared from $Cu(NO_3)_2$ and $Pb(NO_3)_2$ in distilled, deionized water that contained a few drops of 0.1 mol·L^{-1} HNO_3 to prevent the precipitation of Cu(II) and Pb(II) by hydrolysis. The solutions were diluted as required to obtain working solutions in the range of (0.0787 to 2.52) mmol·L^{-1} for Cu(II) and (0.290 to 3.38) mmol·L^{-1} for Pb(II), respectively. The initial pH of the working solutions was adjusted to 4.0 by addition of HNO_3 or NaOH solution, except the experiment examining the effect of pH. Fresh dilutions were used for each sorption study.

2.3. Mineral Identification. Photomicrography of the exterior surface of uncoated zeolite and MOCZ was obtained by SEM (JEOL6335F-SEM, Japan). The distribution of elemental concentrations for the solid sample can be analyzed using the mapping analysis of SEM/EDAX (JEOL SEM (JSM-6301)/OXFORD EDX, Japan). The existence of Cu(II) and Pb(II) ions on the surface of MOCZ was also confirmed by using EDAX. Samples for EDAX analysis were coated with a thin carbon film in order to avoid the influence of any charge effect during the SEM operation. The samples of MOCZ and MOCZ with copper/lead ions adsorbed were also analyzed by X-ray photoelectron spectroscopy (XPS) (ESCA3600 Shimduz).

2.4. Specific Surface Area and Pore Size Distribution Analyses. Analyses of the physical characteristics of MOCZ include specific surface area and pore size distributions. The specific surface area of MOCZ and pore volumes were tested

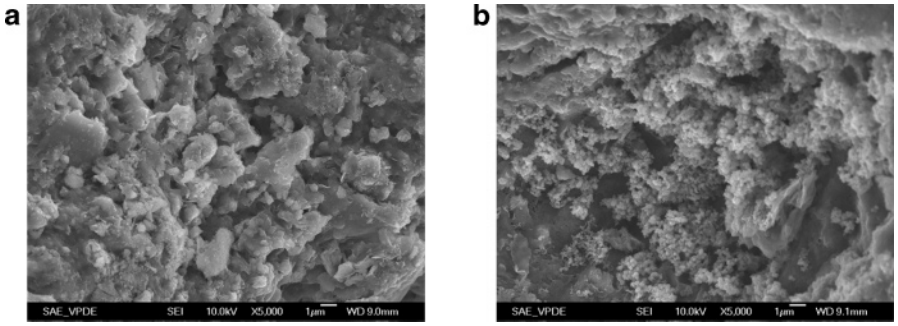

Figure 1. SEM micrograph of samples: (a) zeolite; (b) MOCZ.

using the nitrogen adsorption method with a NOVA 1000 high-speed, automated surface area and pore size analyzer (Quantachrome Corporation, U.S.), and the BET adsorption model was used in the calculation. Calculation of pore size followed the method of BJH according to implemented software routines.

2.5. Methods of Adsorption Studies. Batch sorption experiments were carried out by shaking the flasks at 120 rpm for a period of time using a water bath cum mechanical shaker. Following a systematic process, the sorption uptake capacity of Cu(II) and Pb(II) in batch system was studied in the present work.

2.5.1. Effect of pH. The effect of pH on the adsorption capacity of MOCZ (particle size 20 to 40 mesh) was investigated using solutions of 0.315 mmol·L^{-1} Cu(II) and 0.483 mmol·L^{-1} Pb(II) for a pH range of (1.7 to 6.5) at 288 K. An aliquot of MOCZ (2.0 g·L^{-1}) was added to 20 mL of Cu(II) and Pb(II) solutions. Experiments could not be performed at higher pH values due to hydrolysis of the metal ions. Flasks were agitated on a shaker for 180 min to ensure that equilibrium was reached. The reaction mixture was filtered to separate the MOCZ from the solution. The concentration of free metal ions in the filtrate was analyzed using flame atomic absorption spectrometry (AAS) (AAanalyst 300, Perkin-Elmer). The pH of the solutions at the beginning and end of experiments was also measured. All the experiments were replicated at least once, and only the average values are reported.

2.5.2. Effect of MOCZ Concentration. Batch sorption tests were done at different MOCZ (20 to 40 mesh) concentrations (1 to 8) g·L^{-1} at a constant pH (4.0), contact time (180 min), and temperature (288 K). The initial concentrations of copper and lead were 0.315 mmol·L^{-1} and 0.483 mmol·L^{-1}, respectively. After sorption equilibrium was attained, the concentrations of the metal ions in the filtrate were determined by AAS.

2.5.3. Equilibrium Studied. The equilibrium sorption experiments were carried out at a pH of 4.0 by adding 2.0 g·L^{-1} of MOCZ (20 to 40 mesh) into 20 mL of the solution containing the metal ions with the initial concentrations varying from (0.0787 to 2.52) mmol·L^{-1} and (0.290 to 3.38) mmol·L^{-1} for Cu(II) and Pb(II), respectively. The temperature was controlled with a water bath at a temperature range from 288 to 318 K. After 180 min, the aqueous phase was separated from MOCZ, and the concentration of the metal ions in the aqueous phase was measured.

The amount of adsorbed Cu(II) and Pb(II) ions per gram MOCZ was obtained using the following expression:

$$q_e = v(C_0 - C)/m \tag{10}$$

where q_e is the amount of metal ions adsorbed on the MOCZ (mmol·g^{-1}), C_0 and C are the concentrations of metal ions in the solution (mmol·L^{-1}) prior to and after adsorption, v is the volume of the aqueous phase (L), and m is the dry weight of the sorbent (g).

3. Results and Discussion

3.1. Mineralogy of MOCZ. The SEM photographs in Figure 1 were taken at 5000× magnification to observe the surface morphology of zeolites and MOCZ, respectively. The surface coverage of zeolites by manganese oxides can be observed by comparing the images of virgin (Figure 1a) and MOCZ (Figure 1b). The coated zeolite surfaces were apparently occupied by newborn manganese oxides, which were formed during the coating process. Figure 1b also shows manganese oxides, formed in clusters, apparently on occupied surfaces. At the micron scale, the synthetic coating is composed of small particles on top of a more consolidated coating. In some regions, individual particles of manganese oxides (diameter (2 to 3) μm) appear to be growing in clumps in surface depressions and coating cracks.

3.2. SEM/EDAX Analysis. In conjunction with electron microscopy, elemental identifications of surface features were performed by qualitative EDAX analysis. The EDAX spectrum for MOCZ is illustrated in Figure 2a. There are Mn, Si, O, Al, K, Ca, and Fe signals that can be observed, these being the principal elements of MOCZ. EDAX analysis yields indirect evidence for the mechanism of manganese oxide on the surface of MOCZ. If the solid sample of MOCZ causes a change of elemental constitution through the adsorption reaction, it can be interfered that the manganese oxide has already brought about a chemical interaction with the adsorbate. The EDAX spectrum for the copper and lead systems are illustrated in Figure 2, panels b and c, respectively. The EDAX analysis reveals copper and lead signals on the surface of MOCZ after adsorption from a metallic ions solution. It can be concluded that copper/lead become one element of the solid sample in this spectrum since copper/lead ions have been chemisorbed on the surface of the MOCZ.

The elemental distribution mapping of EDAX for the sample of MOCZ and MOCZ adsorbed copper and lead ions is illustrated in Figure 3. The bright points represent the signal of a particular element in the solid sample. Manganese was spread over the surface of the coated zeolites (Figure 3a), as were copper or lead ions (Figure 3b,c). Results indicated that manganese permeates the interior of zeolite and that the manganese oxide produces a chemical bond with the copper or lead ions. Thus, manganese, copper, and lead are a constituent part of the solid sample.

3.3. Specific Surface Area and Pore Size Distribution Analyses. The specific surface areas for zeolites and MOCZ under un/adsorbed Pb(II) ions are summarized in Table 1. The surface area of MOCZ increased from (24.87 to 28.23) m^2·g^{-1}

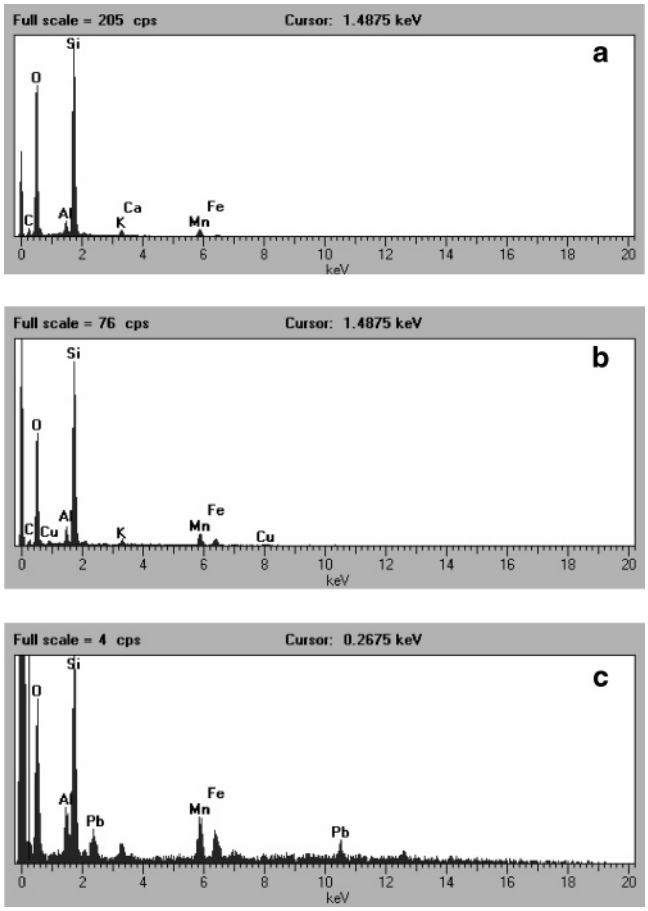

Figure 2. EDAX spectrum of MOCZ: (a) without adsorbing metal, (b) with adsorbed copper ions, (c) with adsorbed lead ions.

Table 1. Specific Surface Areas and Average Pore Diameters for Zeolites and Various MOCZ

	surface area/$m^2 \cdot g^{-1}$	average pore diameter/Å
zeolite	24.87	28.66
unadsorbed[a]	28.23	26.72
adsorbed[b]	27.56	25.91
desorbed[c]	27.70	26.33

[a] Without reacting with Pb(II) ions. [b] After reacting with Pb(II) ions. [c] After soaking with 0.5 $mol \cdot L^{-1}$ acid solution.

after coating manganese oxide on the surface of zeolites, while the average pore diameter decreased from (28.66 to 26.72) Å. After reacting with Pb(II) ions, the pore size distribution of MOCZ had been changed, and parts of pores had disappeared through the adsorption process. The results indicated that parts of pores were occupied with Pb(II) ions and the average pore diameter decreased. Simultaneously, the surface area of the adsorbed MOCZ decreased from (28.23 to 27.56) $m^2 \cdot g^{-1}$. The surface area of the desorbed MOCZ increased, and the average pore diameter also increased after regeneration with acid solution. The results indicated Pb(II) ions could be desorbed from the surface sites of micropores and mesopores.

3.4. Surface Characterization Using the XPS. XPS analyses were performed on samples of MOCZ alone and after reacting with copper or lead ions. The wide scan of MOCZ is presented in Figure 4. It can be noticed that the major elements are manganese, oxygen, and silicon. Detailed spectra of the peaks of oxygen and manganese are shown in Figure 5 and Figure 6a.

Figure 6a shows the binding energies of the observed photoelectron peaks of O1s. It is evident from literature results that the main peak at 529.7 eV is related to the oxygen anions O^{2-} bound to metal cations of the structure. This peak is characteristic of the oxygen in manganese oxides. The second peak at 533.4 eV can be assigned to surface adsorbed oxygen in the form of OH^-.[19]

Manganese oxides are generally expressed with the chemical formula of MnO_x, due to the multiple valence states exhibited by Mn. Therefore, it is reasonable to measure the average oxidation state for a manganese mineral.[19] The observation of the Mn $2p_{3/2}$ peak at 641.9 eV and the separation (11.4 eV) between this and the Mn $2p_{1/2}$ peak indicates that the manganese exhibits an oxidation between Mn^{3+} and Mn^{4+} as shown from the auger plot, but it can be seen from the Mn $2p_{3/2}$ peaks that Mn^{4+} predominates.[20]

From the XPS spectra of the sample of MOCZ reacting with copper ion, Figure 7a shows the binding energies of the observed photoelectron peaks of Cu $2p_{3/2}$ and $2p_{1/2}$. The binding energy of the Cu $2p_{3/2}$ peak at a value of 933.9 eV and a separation of 20.0 eV between the Cu $2p_{3/2}$ and Cu $2p_{1/2}$ peaks show the presence of copper (+2).

The XPS spectra obtained after Pb(II) adsorption on MOCZ is presented in Figure 7b. The figure shows that doublets characteristic of lead appear at 138.3 eV (assigned to Pb $4f_{7/2}$) and at 143.8 eV (assigned to Pb $4f_{5/2}$), respectively, after loading MOCZ with Pb(II) solution. The peak observed at 138.3 eV agrees with the 138.0 eV value reported for PbO.[21] This shows a fixation of lead onto MOCZ during the process. The atomic concentration of oxygen after lead adsorption decreases. Hence, lead adsorption is accompanied by a change in oxygen binding, providing evidence that the oxygen takes part in lead adsorption. The oxygen peak was shifted by 0.80 eV after lead adsorption (Figure 6b). This shift could have been expected since $Pb(OH)_2$ pellets cover the MOCZ surface, it suggests that the oxygen of manganese oxide reacts with the metallic ions.

3.5. Effect of pH on the Sorption of Cu(II) and Pb(II) by MOCZ. The pH of the solution is perhaps the most important parameter for adsorption. The charge of the adsorbate and the adsorbent often depends on the pH of the solution. The manganese oxide surface charge is also dependent on the solution pH due to exchange of H^+ ions. The surface groups of manganese oxide are amphoteric and can function as an acid

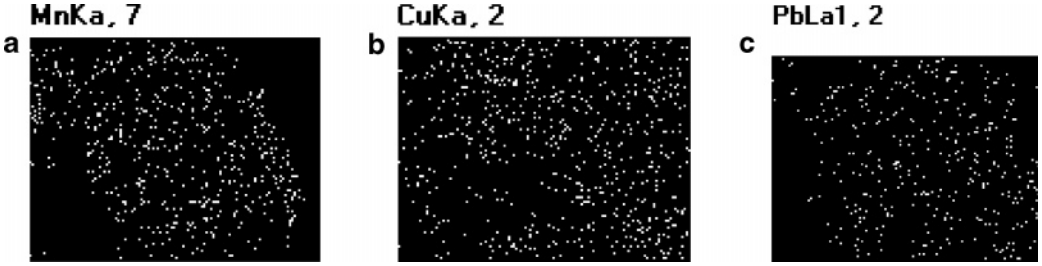

Figure 3. EDAX results of MOCZ (white images in mapping represent the corresponding element): (a) without adsorbing metal, (b) with adsorbed copper ions, (c) with adsorbed lead ions.

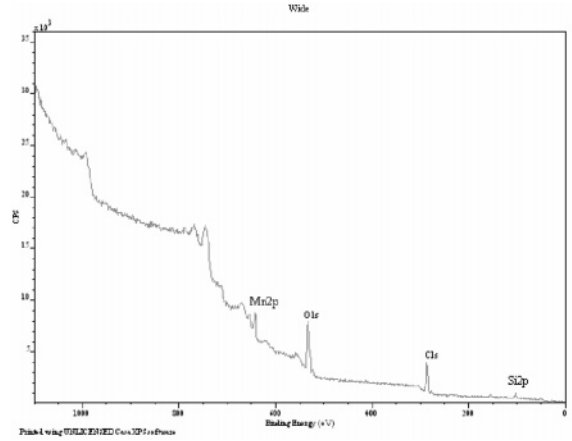

Figure 4. XPS wide scan of MOCZ.

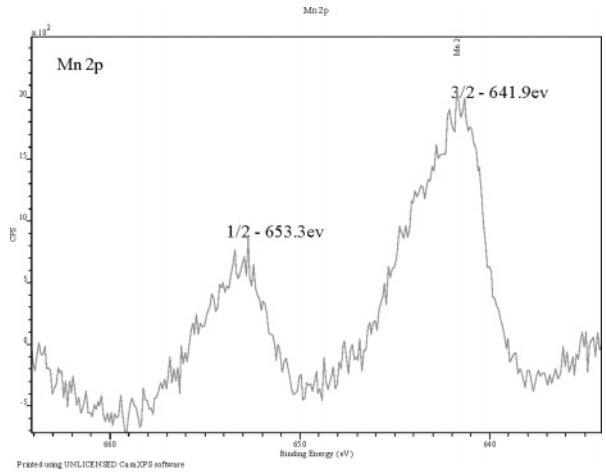

Figure 5. Manganese XPS detailed spectra of MOCZ (Mn $2p_{3/2}$).

or a base.[22] The oxide surface can undergo protonation and deprotonation in response to changes in solution pH.

To understand the adsorption mechanism, the adsorption of Cu(II) and Pb(II) as a function of pH was measured, and the results are shown in Figure 8. The amount of adsorption increased with increasing pH from 2.0 to 6.5 for Cu(II) and pH 1.7 to 3.5 for Pb(II). The adsorption of Pb(II) reached a plateau value at a pH of approximate 3.5. At lower pH values, the small amount of Cu(II) and Pb(II) ions adsorbed is probably due to competitive adsorption of H^+ with metal ions for the exchange site in the system. As the pH increased, the negative charge density on the MOCZ surface increases due to deprotonation of the surface sites on the MOCZ and thus metal ion adsorption increases. The pH of the solution at the end of the experiments was observed to decrease after adsorption by MOCZ. During the adsorption experiment, the pH value of the solution changed from 2.0 to 1.9 and 1.89 and from 6 to 5.1 and 4.8 for Cu(II) and Pb(II), respectively.These results indicate that the mechanism by which Cu(II) and Pb(II) ions were adsorbed onto MOCZ involves an exchange reaction of Cu^{2+} or Pb^{2+} with H^+ on the surface and surface complex formation.

3.6. Effect of MOCZ Concentration on the Sorption of Cu(II) and Pb(II). The adsorption capacity (mmol·g^{-1}) and percentage adsorption of Cu(II) and Pb(II) at different doses of MOCZ are shown in Figure 9. It was observed that the percent of Cu(II) and Pb(II) adsorbed increased from 30 to 85 % and from 50 to 100 %, respectively, when the adsorbent load increased from 1 to 8 g·L^{-1}. It is readily understood that the number of available adsorption sites increases by increasing the adsorbent dose which results in an increase of the amount of adsorbed metal ions. On the other hand, the plot of adsorption capacity versus adsorbent dose reveals that the adsorption capacity was high at lower doses and reduced at higher dose. The primary factor explaining this characteristic is that adsorption sites remain unsaturated during the adsorption reaction whereas the number of sites available for adsorption site increases by increasing the adsorbent dose. The corresponding linear plots of the values of percentage removal (Γ) against dose (m_s) were regressed to obtain expressions for these values in terms of the m_s parameters. This relationship is as follows:

for Cu(II):

$$\Gamma = m_s/(3.19 \times 10^{-2} + 7.96 \times 10^{-3} m_s) \qquad (11)$$

for Pb(II):

$$\Gamma = m_s/(8.63 \times 10^{-3} + 8.65 \times 10^{-3} m_s) \qquad (12)$$

These equations can be used to derive the percentage Cu(II) and Pb(II) adsorbed onto any MOCZ dose within the experimental conditions used in this study due to the high values of correlation coefficient (R) of 0.981 and 0.996 for Cu(II) and Pb(II), respectively.

3.7. Effect of Contact Time at Different Initial Concentrations. The rate of Cu(II) and Pb(II) sorption on MOCZ was determined as a function of the initial metal concentrations. The uptake of metal ions over time at a pH of 4.0 for different initial concentrations of Cu(II) and Pb(II) is shown in Figure 10. It is very clear from the results that the agitation time required for maximum uptake of metal ions was dependent on the initial Cu(II) and Pb(II) concentration. It has been

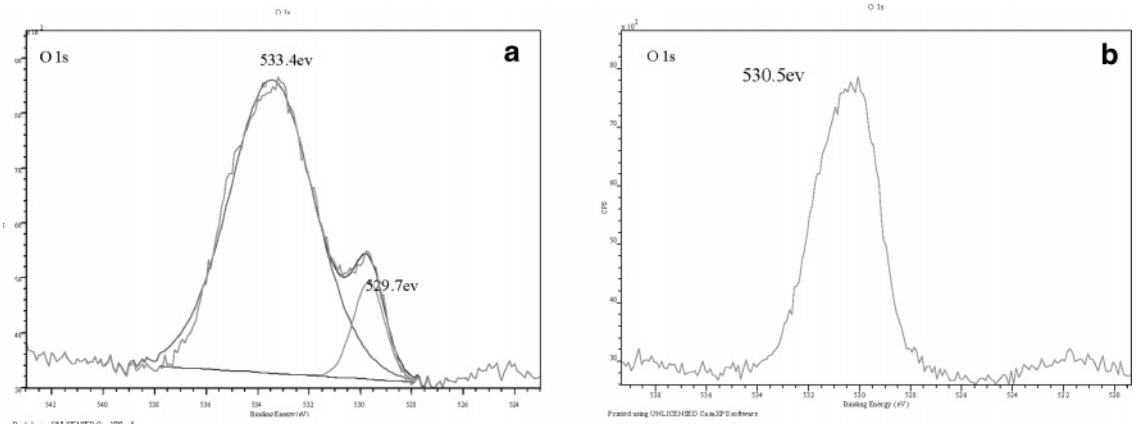

Figure 6. Oxygen XPS spectra of (a) MOCZ and (b) MOCZ reacting with lead ions.

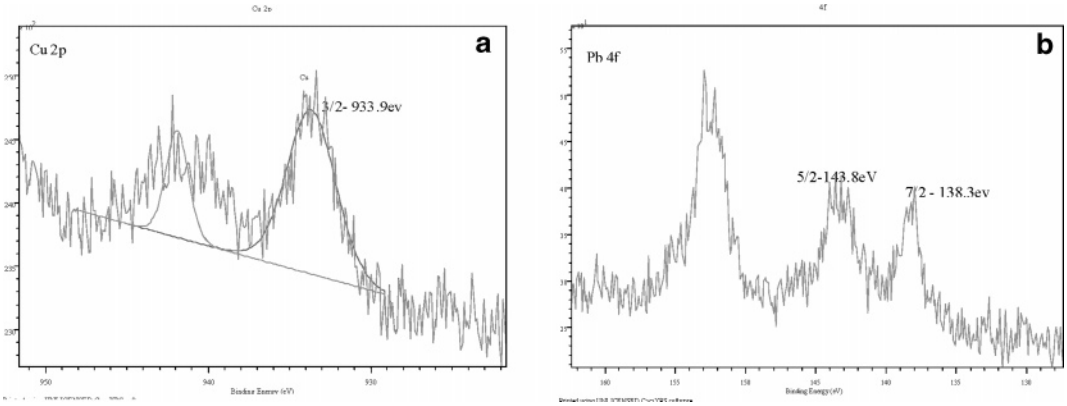

Figure 7. XPS detailed spectra of MOCZ reacting with (a) copper and (b) lead.

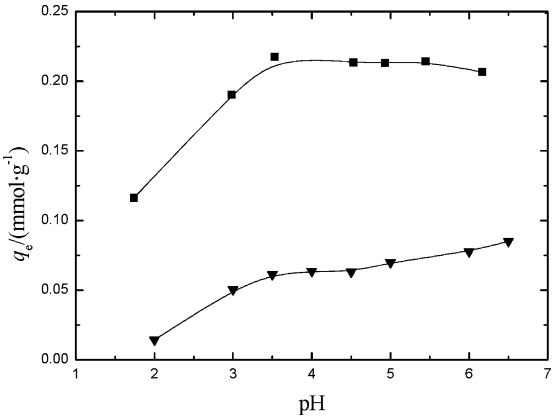

Figure 8. Effect of pH on adsorption of Cu(II) and Pb(II) by MOCZ: ▼, q_e(Cu(II)); ■, qe(Pb(II)).

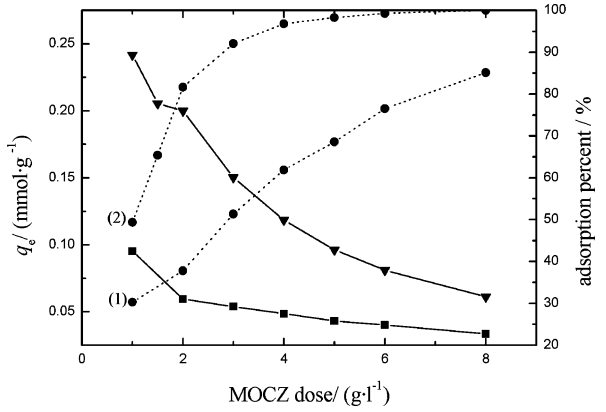

Figure 9. Effect of dosage of MOCZ on Cu(II) and Pb(II) removal. ■, q_e(Cu); ▼, qe(Pb); ●(1), % Cu; ●(2), % Pb.

observed that for all initial concentrations, the adsorption rates are initially rapid due to the readily accessible sites that subsequently became much slower. From Figure 10, it can be seen that equilibrium occurs relatively early in the solution containing the lower metal ions concentrations than the higher ones. The equilibrium time required for maximum removal of Cu(II) was 120, 120, 150, and 180 min when the initial concentration increased from 0.103 to 0.598 mmol·L^{-1}. The removal of Pb(II) was 150, 150, 150, and 180 min when the initial concentration increased from 0.289 to 0.732 mmol·L^{-1}. As a consequence, 180 min was chosen as the reaction time required to reach pseudo-equilibrium in the present "equilibrium" adsorption experiments. It also shows that an increase in metal ion concentration led to an increase in the amount of metal ion adsorbed per unit weight of MOCZ (mmol·g^{-1}). According

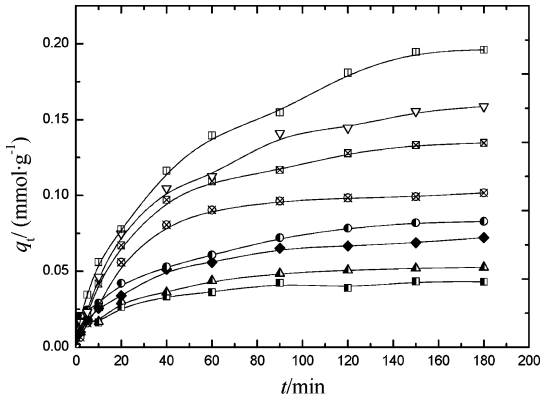

◧,Co(Cu)=0.103 mmol·l^{-1}; ▲,Co(Cu)=0.169 mmol·l^{-1};
◆,Co(Cu)=0.315 mmol·l^{-1}; ◐,Co(Cu)=0.598 mmol·l^{-1};
⊗,Co(Pb)=0.289 mmol·l^{-1}; ⊠,Co(Pb)=0.389 mmol·l^{-1};
▽, Co(Pb)=0.565 mmol·l^{-1}; ◫,Co(Pb)=0.732 mmol·l^{-1}

Figure 10. Effect of contact time on Cu(II) and Pb(II) ions on MOCZ at different initial concentrations.

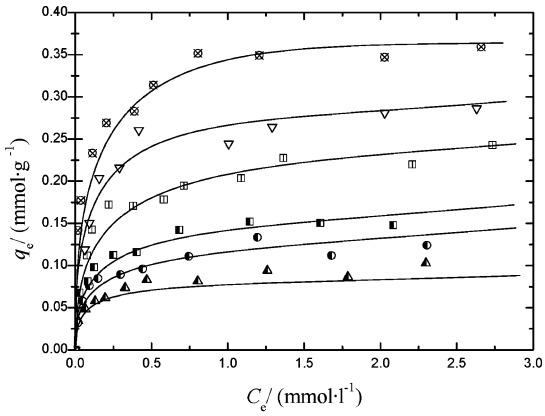

▲,Cu(288K); ◐,Cu(303K); ◧,Cu(318K);
◫,Pb(288K);▽,Pb(303K); ⊗,Pb(318K)

Figure 11. Effect of Cu(II) and Pb(II) concentrations on the adsorption of isotherms of Cu(II) and Pb(II) on MOCZ from aqueous solutions at different temperatures.

to the results of the experiments, the agitation time was fixed at 180 min for the rest of the batch experiments to make sure that equilibrium was reached.

3.8. Effect of Temperature on Cu(II) and Pb(II) Sorption Equilibrium. The equilibrium uptake of Cu(II) and Pb(II) obtained at different temperatures is shown in Figure 11. The

Table 2. Comparison of the Langmuir, Freundlich, Temkin, and Redlich−Peterson Adsorption Constants of Cu(II) and Pb(II) by MOCZ at Different Temperatures

isothermal model parameters	Cu(II)			Pb(II)		
	T/K					
	288	303	318	288	303	318
			Langmuir			
K_a/L·mmol^{-1}	9.11 ± 2.08	13.40 ± 4.13	15.52 ± 4.91	9.68 ± 3.05	13.73 ± 4.04	20.99 ± 5.62
q_m/mmol·g^{-1}	0.104 ± 0.003	0.129 ± 0.003	0.156 ± 0.004	0.241 ± 0.007	0.290 ± 0.005	0.362 ± 0.004
R	0.997	0.998	0.998	0.997	0.998	0.999
p	0.0001	0.0001	0.0001	0.0001	0.0001	0.0001
			Freundlich			
K_F/mmol·g^{-1}	0.087 ± 0.003	0.116 ± 0.007	0.141 ± 0.004	0.203 ± 0.005	0.255 ± 0.013	0.333 ± 0.011
n	4.65 ± 0.36	4.10 ± 0.53	5.13 ± 0.41	5.52 ± 0.59	5.09 ± 0.87	5.38 ± 0.48
R	0.977	0.940	0.979	0.958	0.912	0.969
p	0.0001	0.0001	0.0001	0.0001	0.0006	0.0001
			Temkin			
A/mmol·g^{-1}	0.087 ± 0.002	0.114 ± 0.003	0.141 ± 0.003	0.205 ± 0.004	0.257 ± 0.008	0.332 ± 0.006
B	0.014 ± 0.001	0.018 ± 0.002	0.021 ± 0.002	0.032 ± 0.003	0.041 ± 0.006	0.046 ± 0.003
R	0.979	0.967	0.979	0.970	0.941	0.982
p	0.0001	0.0001	0.0001	0.0001	0.0002	0.0001
			Redlich−Peterson			
K_{RP}	2.76	3.23	4.59	3.17	5.60	11.4
a_{RP}	31.42 ± 1.77	27.34 ± 0.82	32.01 ± 1.64	14.23 ± 0.43	20.35 ± 0.75	33.61 ± 1.58
g	0.948 ± 0.031	0.909 ± 0.015	0.940 ± 0.030	0.949 ± 0.023	0.901 ± 0.026	0.989 ± 0.025
R	0.996	0.999	0.997	0.998	0.997	0.998
p	0.0001	0.0001	0.0001	0.0001	0.0001	0.0001

results show that the temperature effects the uptake of Cu(II) and Pb(II) ions. The adsorption capacities at equilibrium of Cu(II) and Pb(II) increase with increasing temperature in the range 288 to 318 K, indicating that the process of adsorption is endothermic. This was due to the increasing tendency of adsorbate ions to adsorb from the solution to the interface as the temperature increased. Regarding the influence of the initial concentration of metal ions, the adsorption capacities of the MOCZ increased first with the increasing of the initial concentration of Cu(II) and Pb(II) and reached saturation values of around 0.40 and 0.75 mmol·L^{-1} for Cu(II) and Pb(II), respectively. While the initial concentrations of metal ions increasing, the driving force of the concentration gradient increasd.

3.9. Analysis of Equilibrium Model Constants. To optimize the design of a sorption system to remove metal ions from aqueous solutions, four isotherm equations have been used for the equilibrium modeling of these sorption systems: the Langmuir, Freundlich, Temkin, and Redlich−Peterson isotherms.

The Langmuir, Freundlich, Temkin, and Redlich−Peterson adsorption constants evaluated from the isotherms at different temperatures and their correlation coefficients (*R*) are presented in Table 2 according to linear forms of eqs 1, 3, 5, and 7, respectively.

As shown in Table 2, the constants of K_a and q_{max} (K_F) and *A* and *B* (K_{RP}) of the four isotherm models were all increased with increasing temperature. These results indicated that Cu(II) and Pb(II) can be easy uptake by MOCZ from aqueous solutions with high adsorptive capacity and that the adsorptive capacity increased with increasing temperature. The maximum capacity (q_{max}) of MOCZ in this study for Cu(II) and Pb(II) determined from the Langmuir plots was 0.156 mmol·g^{-1} and 0.362 mmol·g^{-1}, respectively, at a temperature of 318 K. The values of *n* of the Freundlich constant for both Cu(II) and Pb(II) obtained at 303 K appear to be lower in comparison with those at the other temperatures. As the constant *n* is greater than unity, this indicates that metal ions are favorably adsorbed by MOCZ at all the temperatures studied.[18] The constants of *g* determined from the Redlich−Peterson isotherm lies between 0 and 1, indicating that the adsorption process studied here can be described by the Redlich−Peterson model. As the values of *g* obtained for Cu(II) and Pb(II) adsorption approach unity for all temperatures studies, the isotherm is approaching the Langmuir form.

It can be concluded from the constants given in Table 2 that the equilibrium data fit the Langmuir and Redlich−Peterson equilibrium models quite well in the studied concentration range of Cu(II) and Pb(II) and at all temperatures studied in the present work. In all cases, the Freundlich isotherm represents the poorest fit of the experimental data. The comparison of the values of *R* indicates that the Langmuir and Redlich−Peterson isotherms best fit the experimental data under all conditions. The fact that the Langmuir isotherm fits the experimental data very well may be due to homogeneous distribution of active sites on the MOCZ surface, since the Langmuir equation assumes that the surface is homogeneous.[18]

The values of q_{max} obtained from the Langmuir isotherm equation for Pb(II) adsorption on MOCZ was greater than that for Cu(II) at all temperatures, which indicates that the functional groups on the surface of MOCZ have a relatively stronger affinity for Pb(II) than Cu(II). The observed affinity in the adsorption of Pb(II) and Cu(II) could be attributed to the difference in their class behavior on the basis of their covalent indices.[23] Lead(II) is classified as a class b ion, while copper-(II) is classified as a borderline ion. In general, the greater the covalent index the greater is the class b character and, consequently, its potential to form covalent bonds with adsorbent ligands. A similar result for cation adsorption has been reported by Heidmann et al.[24]

3.10. Thermodynamic Parameters of Adsorption. To estimate the effect of temperature on the adsorption of Cu(II) and Pb(II) on MOCZ, the free energy change ($\Delta G°$), enthalpy change ($\Delta H°$), and entropy change ($\Delta S°$) were determined. Since K_a is equilibrium constant, its dependence with temperature can be used to estimate both enthalpy and entropy associated to the sorption process. The standard enthalpy and entropy changes of sorption were determined from the $\Delta G°$ versus *T* plot according to eq 9. The results are shown in Table 3.

The negative $\Delta G°$ values of both Cu(II) and Pb(II) ions at various temperatures is due to the fact that the adsorption

Table 3. Thermodynamic Parameters for the Adsorption of Cu(II) and Pb(II) at Various Temperatures by MOCZ

		T/K		
metal ion		288	303	318
Cu(II)	$\Delta G°$/kJ·mol^{-1}	−5.12	−6.29	−6.96
	$\Delta H°$/kJ·mol^{-1}	12.5 ± 2.9		
	$\Delta S°$/J·mol^{-1}·k^{-1}	61.3 ± 9.6		
Pb(II)	$\Delta G°$/kJ·mol^{-1}	−5.18	−6.37	−7.85
	$\Delta H°$/kJ·mol^{-1}	20.5 ± 1.7		
	$\Delta S°$/J·mol^{-1}·k^{-1}	89.0 ± 5.6		

processes are spontaneous and that the negative value of $\Delta G°$ decreased with an increase in temperature, indicating that the spontaneous nature of adsorption of Cu(II) and Pb(II) are inversely proportional to the temperature. Enhancement of adsorption capacity of the adsorbent at higher temperatures may be attributed to an enlargement of pore size and/or activation of the adsorbent surface. Positive values of $\Delta H°$ indicate the endothermic nature of the process. The positive $\Delta S°$ reflects the affinity of the adsorbent material for metal ions, namely, Cu(II) and Pb(II).

Literature Cited

(1) Mohan, D.; Singh, K. P. Single- and multi-component adsorption of cadmium and zinc using activated carbon derived from bagasse—an agricultural waste. *Water Res*. **2002**, *36*, 2304−2318.

(2) Babel, S.; Kurniawan, T. A. Low-cost adsorbents for heavy metals uptake from contaminated water: a review. *J. Hazard. Mater. B* **2003**, *97*, 219−243.

(3) Edwards, M. A.; Benjamin, M. M. Adsorption filtration using coated sand: a new approach for treatment of metal-bearing wastes. *J. Water Pollut. Control Fed*. **1989**, *61*, 1523−1533.

(4) Al-Degs, Y.; Khraisheh, M. A. M. The feasibility of using diatomite and Mn-diatomite for remediation of Pb^{2+}, Cu^{2+}, and Cd^{2+} from water. *Sep. Sci. Technol*. **2000**, *35*, 2299−2310.

(5) Kuan, W. H.; Lo, S. L.; Wang, M. K. Removal of Se(IV) and Se(VI) from water by aluminum oxide coated sand. *Water Res.* **1998**, *32*, 915−923.

(6) Al-Haj Ali, A.; El-Bishtawi, R. Removal of lead and nickel ions using zeolite tuff. *J. Chem. Technol. Biotechnol*. **1997**, *69*, 27−34.

(7) Fritsch, S.; Post, J. E.; Navrotsky, A. Energetics of low-temperature polymorphs of manganese dioxide and oxyhydroxide. *Geochim. Cosmochim. Acta*. **1997**, *61*, 2613−2616.

(8) Tamura, H.; Katayama, N.; Furrich, R. The Co^{2+} adsorption properties of Al_2O_3, Fe_2O_3, Fe_3O_4, TiO_2, and MnO_2 evaluated by modeling with the Frumkin isotherm. *J. Colloid Interface Sci*. **1997**, *195*, 192−202.

(9) Fu, G.; Allen, H. E.; Cowan, C. E. Adsorption of cadmium and copper by manganese oxide. *Soil Sci*. **1991**, *152*, 72−81.

(10) Catts, J. G.; Langmuir, D. Adsorption of Cu, Pb, and Zn by δ-MnO_2: applicability of the side binding-surface complexation model. *Appl. Geochem*. **1986**, *1*, 255−264.

(11) Birsen, A.; Timothy, A. D. Application of MnO_2 coated scintillating and extractive scintillating resins to screening for radioactivity in groundwater. *Nucl. Instrum. Methods. Phys. Res., Sect. A* **2003**, *505*, 458−461.

(12) Kanungo, S. B.; Paroda, K. M. Interfacial behavior of some synthetic MnO_2 samples during their adsorption of Cu^{2+} and Ba^{2+} from aqueous solution at 300 K. *J. Colloid Interface Sci*. **1984**, *98*, 252−260.

(13) Liu, D. F.; Teng, Z.; Sansalone, J. J.; Cartledge, F. K. Surface characteristics of sorptive-filtration storm water media. II. Higher specific gravity (ρ_s > 1.0) oxide-coated fixed media. *J. Environ. Eng*. **2001**, *127*, 879−888.

(14) Langmuir, I. The constitution and fundamental properties of solids and liquids. *J. Am. Chem. Soc*. **1916**, *38*, 2221−2295.

(15) Freundlich, H. M. F. Uber die adsorption in lasungen. *Z. Phys. Chem*. **1906**, *57*, 385−470.

(16) Guibal, E.; Saucedo, I.; Roussy, J. Uptake of uranyl ions by new sorbing polymers: discussion of adsorption isotherms and pH effect. *React. Polym.* **1994**, *23*, 147−156.

(17) Redlich, O.; Peterson, D. L. A useful adsorption isotherm. *J. Phys. Chem*. **1959**, *63*, 1024.

(18) Aksu, Z. Determination of the equilibrium, kinetic and thermodynamic parameters of the batch biosorption of lead(II) ions onto *Chlorella vulgaris*. *Process Biochem*. **2002**, *38*, 89−99.

(19) Katsoyiannis, I. A.; Zouboulis, A. I. Biological treatment of Mn(II) and Fe(II) containing groundwater: kinetic considerations and product characterization. *Water Res*. **2004**, *38*, 1922−1932.

(20) Mirzaei, A. A.; Shaterian, H. R.; Kaykhaii, M. The X-ray photoelectron spectroscopy of surface composition of aged mixed copper manganese oxide catalysts. *Appl. Surf. Sci.* **2005**, *239*, 246−254.

(21) Taty-Costodes, V. C.; Fauduet, H.; Porte, C.; Delacroix, A. Removal of Cd(II) and Pb(II) ions, from aqueous solutions, by adsorption onto sawdust of *Pinus sylvestris*. *J. Hazard. Mater*. *B* **2003**, *105*, 121−142.

(22) Davies, S. H. R.; Morgan, J. J. Manganese(II) oxidation kinetics on metal oxide surfaces. *J. Colloid Interface Sci*. **1989**, *129*, 63−77.

(23) Nieboer, E.; McBryde, W. A. E. Free-energy relationships in coordination chemistry. III. A comprehensive index to complex stability. *Can. J. Chem*. **1973**, *51*, 2512−2524.

(24) Heidmann, I.; Christl, I.; Leu, C.; Kretzschmar, R. Competitive sorption of protons and metal cations onto kaolinite: experiments and modeling. *J. Colloid Interface Sci*. **2005**, *282*, 270−282.

Received for review September 30, 2005. Accepted January 20, 2006. The authors express their sincere gratitude to Henan Science and Technology Department and the Education Department of Henan Province in China for the financial support of this study.

JE0504008